Radiotherapy and Oncology 107 (2013) 377–381

Contents lists available at SciVerse ScienceDirect

Radiotherapy and Oncology

journal homepage: www.thegreenjournal.com

Secondart cancer after prostate

Early biomarkers related to secondary primary cancer risk in radiotherapy treated prostate cancer patients: IMRT versus IMAT ☆

Joke Werbrouck [a], Piet Ost [b], Valerie Fonteyne [b], Gert De Meerleer [b], Wilfried De Neve [b], Evelien Bogaert [b], Laurence Beels [a], Klaus Bacher [a], Anne Vral [a], Hubert Thierens [a,*]

[a] Department of Basic Medical Sciences, Ghent University; and [b] Department of Radiation Oncology, Ghent University Hospital, Gent, Belgium

ARTICLE INFO

Article history:
Received 18 March 2013
Received in revised form 3 May 2013
Accepted 6 May 2013
Available online 19 June 2013

Keywords:
Secondary cancer risk
IMRT
Rotational radiation therapy
γH2AX foci
Micronuclei

ABSTRACT

Purpose: To investigate whether rotational techniques (Volumetric Modulated Arc Therapy – VMAT) are associated with a higher risk for secondary primary malignancies compared to step-and-shoot Intensity Modulated Radiation Therapy (ss-IMRT). To this end, radiation therapy (RT) induced DNA double-strand-breaks and the resulting chromosomal damage were assessed in peripheral blood T-lymphocytes of prostate cancer (PCa) patients applying γH2AX foci and G_0 micronucleus (MN) assays.
Methods and materials: The study comprised 33 PCa patients. A blood sample was taken before start of therapy and after the 1st and 3rd RT fraction to determine respectively the RT-induced γH2AX foci and MN. The equivalent total body dose (D_{ETB}) was calculated based on treatment planning data.
Results: A linear dose response was obtained for γH2AX foci yields versus D_{ETB} while MN showed a linear-quadratic dose response. Patients treated with large volume (LV) VMAT show a significantly higher level of induced γH2AX foci and MN compared to IMRT and small volume (SV) VMAT ($p < 0.01$). Assuming a linear-quadratic relationship, a satisfactory correlation was found between both endpoints (R^2 0.86).
Conclusions: Biomarker responses were governed by dose and irradiated volume of normal tissues. No significant differences between IMRT and rotational therapy inherent to the technique itself were observed.

 Radiotherapy and Oncology 107 (2013) 377–381

Radiation therapy (RT) is a cornerstone of cancer management [1]. However, Hall and Wuu stated that "radiation is a two-edged sword: it is the major modality to treat cancer, but it can also be the cause of cancer" [2]. As contemporary techniques are able to deliver higher doses more precisely ('image-guided radiotherapy' (IGRT)), the therapeutic ratio of RT increases. Consequently, the cure rates increase and the issue of the development of radiation induced secondary malignancies (RISM) becomes more important [3,4].

Compared to 3D conformal RT (3DCRT) IMRT is hypothesised to increase the risk for RISM because it requires more radiation fields involving a larger volume of normal tissue exposed to low radiation doses and because it requires more monitor units (MU) to deliver a specified dose causing a larger total body dose due to head leakage and collimator scatter [2,3,5]. Using Volumetric Modulated Arc Therapy (VMAT), dose rate, shape of the beam and speed of rotation can be changed during gantry rotation enabling to give the RT fraction in one single rotation. Variations on the VMAT principle are RapidArc (Varian Medical Systems, Inc., Palo Alto, CA, USA) and IMAT (Intensity Modulated Arc Therapy) [6]. No information is available regarding RISM following arc therapy.

In this paper, a biomarker approach is applied to compare the potential risk for radiation induced RISM in prostate cancer (PCa) patients treated with ss-IMRT and VMAT (small volume and high volume). To this end RT induced DNA double-strand-breaks (γH2AX foci) and the resulting chromosomal damage (MN) were assessed in PBLs.

Materials and methods

Patient population and blood sampling

The study population consisted of 33 PCa patients treated at the Department of Radiation Oncology (Ghent University Hospital, Belgium) between October 2010 and August 2011. Heparinised blood samples were obtained from patients treated with 3 different RT modalities: (1) ss-IMRT (Elekta Synergy linear accelerator) ($n = 12$), (2) small volume (SV) VMAT (RapidArc; Varian Clinac linear accelerator) ($n = 9$) and (3) large volume (LV) VMAT (IMAT;

* Corresponding author. Address: Department of Basic Medical Sciences, Ghent University, Proeftuinstraat 86, 9000 Gent, Belgium.
E-mail address: Hubert.Thierens@ugent.be (H. Thierens).

0167-8140/$ - see front matter © 2013 The Authors. Elsevier Ireland Ltd. All rights reserved.
http://dx.doi.org/10.1016/j.radonc.2013.05.014

Table 1
Overview of patient population and treatment modalities considered in this study.

RT technique		Age	MU/fraction	Photon energy (MV)	PTV (dm^3)	Dose/fraction (Gy)	Total tumour dose (Gy)
IMRT	Mean	61.6	328.9	6	0.136	2.09	78.03
	Range	47.5–72.2	305–379		0.086–0.160	1.92–2.25	69.12–85.50
SV-VMAT	Mean	64.9	378.8	6	0.137	2.02	75.58
	Range	50.8–77.3	322–468		0.062–0.211	2.00–2.10	72.00–77.67
LV-VMAT	Mean	64.8	428.1	18	0.231	1.83	65.22
Normofractionation	Range	57.6–73.5	275–734		0.083–1.048	1.27–2.09	45.00–75.90
LV-VMAT	Mean	67.7	733.8	18	0.17	2.85	71.19
Hypofractionation	Range	60.5–77.3	532–1064		0.138–0.203	2.83–2.87	70.75–71.75

Abbreviations: MU, number of monitor units; MV, mega voltage; PTV, planned target volume; Gy, gray.

Elekta SL18 linear accelerator). The latter population was further subdivided in a group receiving normofractionation ($n = 8$) and a group receiving hypofractionation ($n = 4$). In these groups the dose per fraction was respectively 2.09, 2.02, 1.83 and 2.85 Gy. Details regarding patient population and treatment modalities are summarised in Table 1. Before each fraction, imaging was applied to verify position of patient and fields: Electronic Portal Imaging Device (EPID) for LV-VMAT and Cone Beam Computed Tomography (CBCT) for ss-IMRT and SV-VMAT. After obtaining signed informed consent, blood samples were taken at different time points, as shown in Fig. 1. Blood samples taken a few minutes after exposure reflect the average dose given to the lymphocyte pool in the peripheral blood [7]. Blood sampling for the γH2AX foci was performed before and after the first fraction, blood sampling for the MN assay was performed before and after the third fraction. In previous work it was shown that the number of radiation induced MN is proportional to the equivalent total body dose (D_{ETB}) up to three fractions of RT treatment [8].

γH2AX foci and G_0 MN assays

The procedure for the γH2AX foci assay on T-lymphocytes is described in detail in a previous paper [9]. The Metacyte software module of the Metafer 4 scanning system (MetaSystems, Altlussheim, Germany) was applied for automated scanning of the slides, for spot detection and foci scoring [10].

The procedure for the G_0 MN assay can be found elsewhere [11]. The MSearch software module of the Metafer 4 scanning system (MetaSystems) was applied for automated scanning of binucleated (BN) cells and scoring of MN. Gallery images of the positive as well as the negative class of BN cells were checked and scores were adjusted when necessary.

In vitro irradiations

For the determination of the γH2AX foci and MN *in vitro* dose response curves, whole blood samples of 3 healthy donors were exposed to different doses up to 500 mGy of Co-60 γ-rays. The same procedures as used for the patient samples were applied.

Calculation of the equivalent total body dose

The equivalent total body dose D_{ETB} was calculated for each patient based on the treatment planning data. To this end the mean dose within the skin contour of the scanned volume was normalised to the patient mass. For the γH2AX foci assay D_{ETB} has to be interpreted as the equivalent total body blood dose. As liver, heart/large blood vessels and lungs contain together 38.5% of the total blood volume it was assumed that 61.5% of the blood pool is distributed uniformly over the rest of the body. In the D_{ETB} calculation the contribution of the medical imaging, CBCT and EPID was also taken into account.

Statistical analysis

Statistical analysis of the data was performed using the Statistical Package for Social Sciences (SPSS) version 20.0. The 2-tailed Mann–Whitney test was performed to investigate the significance of differences in biomarker scores. The statistical power of the obtained results was assessed using G∗Power version 3.1.4 software [12].

Results

γH2AX foci and MN induced in vivo by different RT modalities for prostate cancer

Fig. 2 represents the number of radiation induced (background corrected) γH2AX foci/T-lymphocyte plotted against D_{ETB} after one RT fraction for each patient. Taking into account all foci data, the number of γH2AX foci increases linearly with D_{ETB} but with a relatively large scatter of the data (R^2 0.67). For the IMRT patient group two separated clouds of data points can be noticed in the dose ranges 0–20 mGy and 40–60 mGy. Compared to the *in vitro* dose response patient foci-D_{ETB} data are generally higher, especially for the hypofractionated LV-VMAT. However, differences are not statistically significant (p 0.12).

The mean values of D_{ETB}/fraction and number of radiation induced γH2AX foci averaged over the patients for each RT technique applied are summarised in Table 2 and represented graphically in Fig. 2 by the × symbols with standard deviations as error bars. The

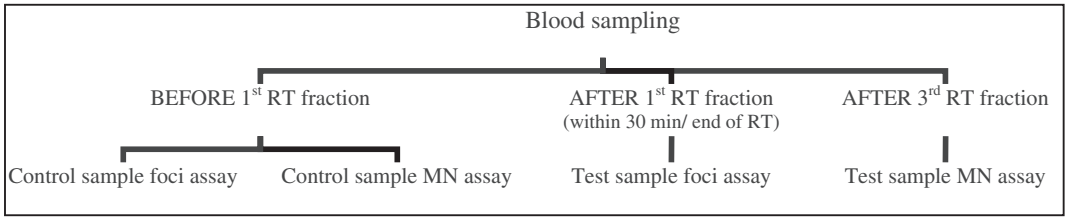

Fig. 1. Time schedule of the blood samplings of the study.

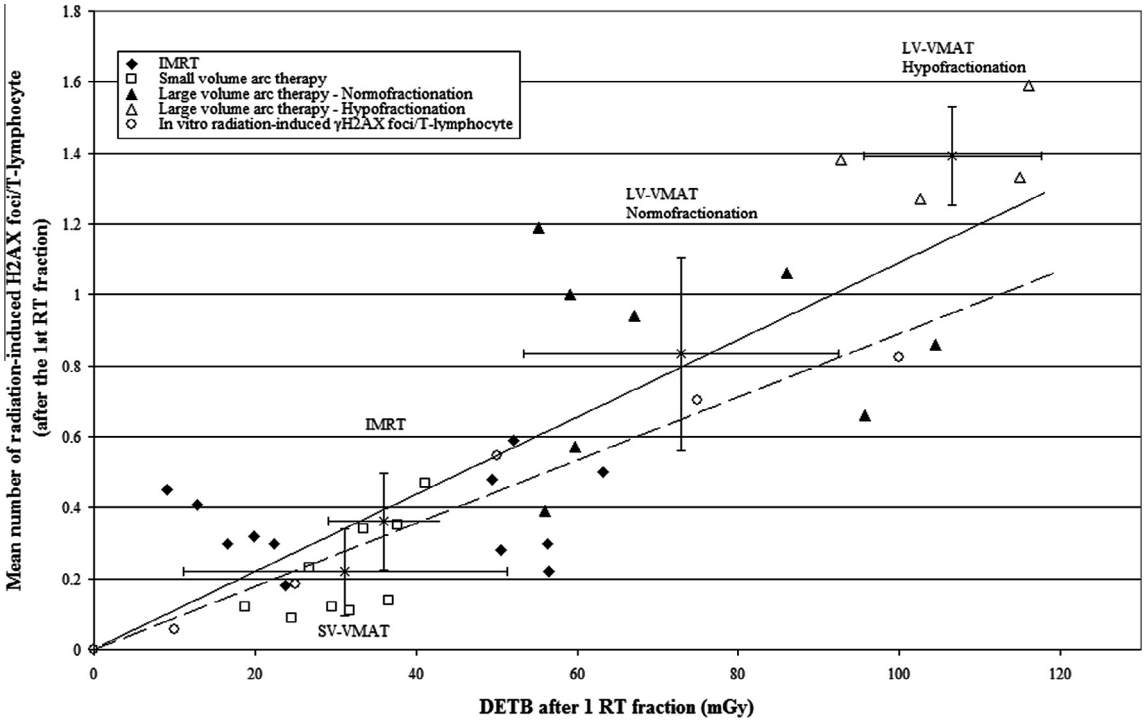

Fig. 2. γH2AX foci/T-lymphocyte induced (background corrected) by the first fraction of RT as a function of D_{ETB}. The full line represents a linear fit to all *in vivo* data (R^2 0.67). The open circles represent the number of γH2AX foci/T-lymphocyte after *in vitro* irradiation of whole blood. The dashed line represents the linear regression through the *in vitro* data points.

Table 2
Mean values of D_{ETB} after 1 and 3 fractions, mean number of radiation induced γH2AX foci and mean number of radiation-induced MN/1000BN averaged over the patients for each RT technique applied.

	D_{ETB}/fraction (mGy)		γH2AX foci/T-lymphocyte		D_{ETB}/3 fractions (mGy)		MN/1000BN	
	Mean (SD)	Range (mGy)	Mean (SD)	Range	Mean (SD)	Range	Mean (SD)	Range
IMRT[a]	36.06 (20.11)	9.14–63.13	0.36	0.18–0.59	87.34 (53.27)	34.80–176.69	2	−5 to 10
CBCT	3.93				19.17			
Low volume arc therapy[a]	31.18 (7.03)	18.83–37.77	0.22	0.09–0.47	96.26 (21.11)	61.70–128.61	7	−1 to 14
CBCT	2.77				13.51			
High volume arc therapy[a] (Normofractionation)	72.92 (19.61)	55.19–104.48	0.83	0.39–1.19	225.07 (58.82)	171.88–319.73	26	8–64
EPID	5.2				21.9			
High volume arc therapy[a] (Hypofractionation)	106.59 (11.09)	92.74–116.09	1.39	1.27–1.59	326.09 (33.27)	284.53–354.56	53	41–65

Abbreviations: D_{ETB}, equivalent total body dose; CBCT, Cone Beam Computed Tomography; EPID, Electronic Portal Imaging Device.
[a] Including the CBCT/EPID dose contribution.

number of γH2AX foci was borderline significantly higher in IMRT compared to SV VMAT which is in line with the D_{ETB} values (p 0.039). On the other hand the mean number of foci induced by LV-VMAT was significantly higher compared to both IMRT and SV-VMAT ($p < 0.001$). Significance remains even when the LV-VMAT patients are subdivided according to the normo- and hypofractionation regime ($0.001 < p < 0.005$). The same trend is seen for the D_{ETB} values. The statistical significance of differences in foci numbers obtained among these rather small patient populations was supported by a post hoc power analysis which indicated a very good power (range 0.916–0.999) except for the comparison between IMRT and SV-VMAT (0.512).

In Fig. 3 the number of MN/1000BN induced in patients' PBLs are plotted versus D_{ETB} after the 3rd fraction for all patients. The number of radiation induced MN (background corrected) shows a linear-quadratic response as a function of the calculated D_{ETB} (R^2 0.64). *In vitro* irradiation of whole blood clearly results in lower MN yields than observed for the RT patients and calculated D_{ETB}. This difference in MN dose response is significantly different (p 0.021). The mean number of radiation-induced MN/1000BN and mean D_{ETB} after the 3rd fraction of RT averaged over patients for the different modalities are also given in Table 2 and represented by the × symbols in Fig. 3. LV-VMAT results in significantly higher values compared to both IMRT and SV-VMAT ($p < 0.001$). The significance of the difference holds when the LV-VMAT group is subdivided according to normo- and hypofractionation schedule. LV-VMAT hypofractionation (mean tumour dose per fraction of 2.85 Gy) even showed twice as much MN formation as normofractionation (mean tumour dose per fraction of 1.83 Gy).

MN versus γH2AX foci

The correlation between the number of radiation induced (background corrected) MN/1000BN and γH2AX foci/1000 T-lymphocytes for the patient population is represented in Fig. 4. A linear-quadratic relationship between both biomarkers of radiation damage results in an excellent fit (R^2 0.86). The mean baseline level of the γH2AX foci was 0.15 ± 0.14 and for the MN was 17.45 ± 5.82. No correlation between the baseline levels of both biomarkers could be demonstrated (R^2 0.07).

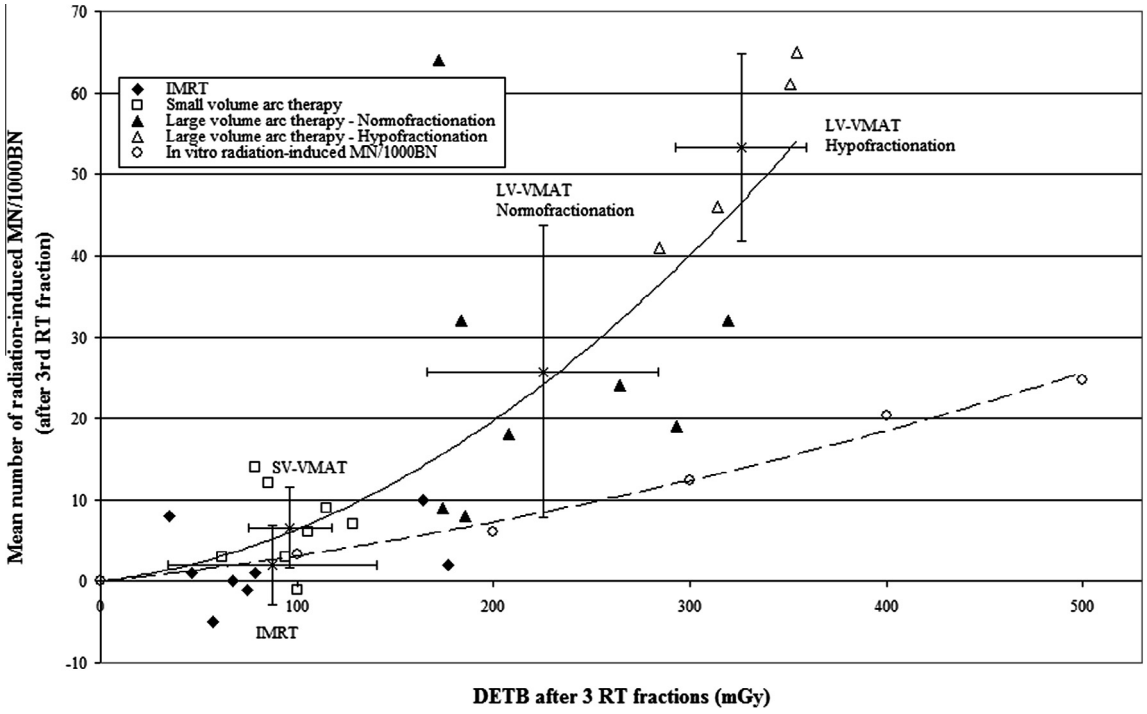

Fig. 3. Radiotherapy induced (background corrected) MN per 1000 binucleated cells (MN/1000BN) after the third fraction as a function of D_{ETB}. The full line represents a linear-quadratic fit to all data points (R^2 0.64). The open circles represent the number of MN/1000BN after *in vitro* irradiation of whole blood. The dashed line represents the linear-quadratic fit through the *in vitro* data points.

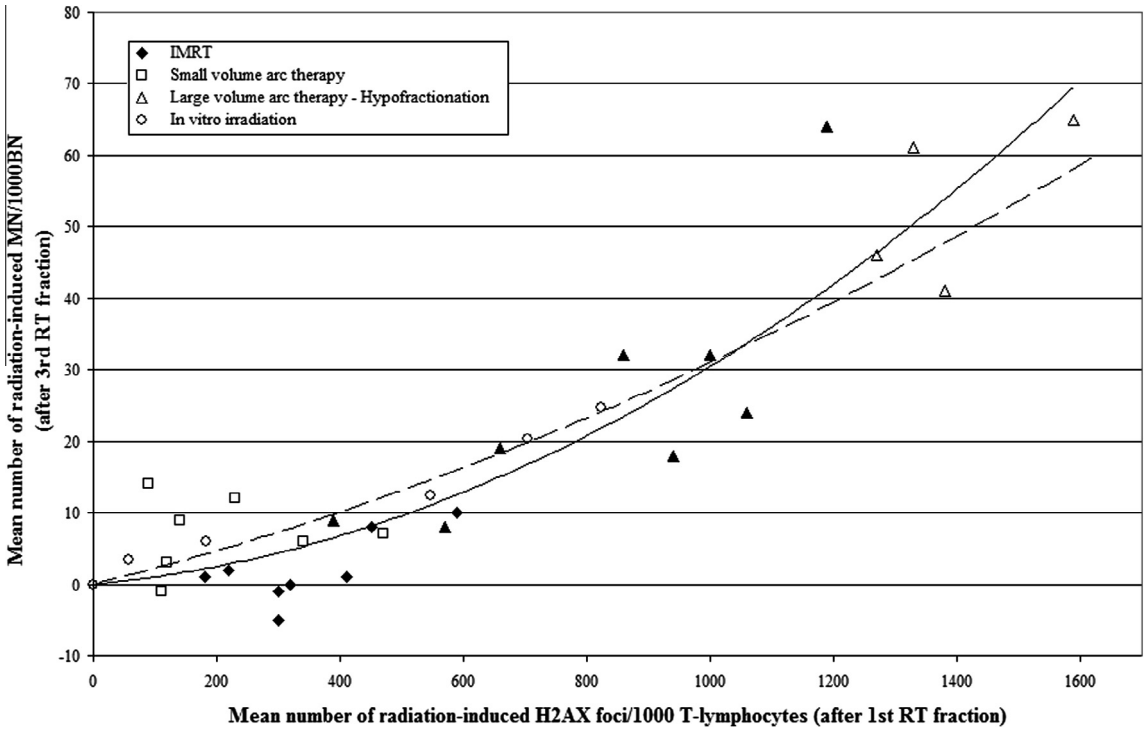

Fig. 4. Radiotherapy induced (background corrected) MN expressed as MN/1000BN after the 3rd fraction as a function of the number of radiotherapy-induced (background corrected) foci per 1000 T-lymphocytes after the 1st fraction. The full line represents a linear-quadratic fit through the *in vivo* data points (R^2 0.86). The dashed line represents a linear-quadratic fit through the *in vitro* data points (R^2 0.97).

Discussion

In present study, a biomarker approach was used to compare the risk for development of RISM in PCa patients receiving ss-IMRT, SV-VMAT and LV-VMAT in a normo- and hypofractionation regime. The patients' γH2AX foci and MN data show in general a systematic increase with D_{ETB}. Foci yields were borderline significantly higher in IMRT compared to SV-VMAT treated patients but in line with the D_{ETB} values. It is often stated that SV-VMAT reduces the daily treatment time compared to IMRT resulting in a smaller

amount of scatter radiation from the treatment head, which should lower the risk of RISM [13]. On the other hand Aznar et al. indicated that the mean dose to healthy tissues was slightly increased for SV-VMAT treatment compared to 5-field IMRT [13,14]. Our data do not indicate a significant difference in risk of RISM inherent to the technique itself.

For IMRT treated patients, receiving a D_{ETB}/fraction less than 20 mGy, the number of observed γH2AX foci was 3–5× higher than expected from the *in vitro* dose–response. A comparison of the low dose IMRT data with the *in vivo* dose response determined over the total dose range resulted in a borderline significant difference (p 0.046). Possible explanations are underestimation of D_{ETB} by low dose radiation scatter and/or head leakage not included in the calculation of D_{ETB} or the bystander effect [15,16]. Such an effect was not observed for the micronuclei and also not for the *in vitro* irradiated samples.

A systematic comparison of *in vivo* and *in vitro* data shows higher scores for both biomarkers after *in vivo* exposure especially for LV-VMAT produced by 18 MV X-rays. This difference may be explained by the factors just mentioned but for the LV-VMAT data also photo-neutrons, which have a high RBE, may play a role [5].

The used biomarkers can also be considered as early biomarkers of secondary cancer risk after RT. In a radiosensitive Patched-1 mouse model γH2AX foci induced in shielded cerebellum of mice irradiated *in vivo* were linked to medulloblastoma formation [17]. MN as marker for chromosomal damage are linked to carcinogenesis due to the causal role of balanced chromosome rearrangements in early stages of carcinogenesis and the increased MN frequency seen in cancer patients [18].

Conclusion

A comparative study of γH2AX foci and MN as radiation effect biomarkers in PCa patient groups treated with IMRT and VMAT (small and large volume) reveals that the biomarker response was governed by dose and irradiated volume of normal tissue However, no significant differences between IMRT and rotational therapy inherent to the technique itself were observed.

Conflict of interest

None of the authors have conflicts of interests to report concerning the manuscript.

Acknowledgements

We are grateful to all patients for their participation. The Federal Agency for Nuclear Control is acknowledged for financial support.

References

[1] Mohanti BK, Bansal M. Late sequelae of radiotherapy in adults. Support Care Cancer 2005;13:775–80.
[2] Hall EJ, Wuu C. Radiation-induced second cancers: the impact of 3D-CRT and IMRT. Int J Radiat Oncol Biol Phys 2003;56:83–8.
[3] Hall EJ, Phil D. Intensity-modulated radiation therapy, protons and the risk of second cancers. Int J Radiat Oncol Biol Phys 2006;65:1–7.
[4] Kry SF, Salehpour M, Followill DS, et al. The calculated risk of fatal secondary malignancies from intensity-modulated radiation therapy. Int J Radiat Oncol Biol Phys 2005;62:1195–203.
[5] Newhauser WD, Durante M. Assessing the risk of second malignancies after modern radiotherapy. Nat Rev Cancer 2011;11:438–48.
[6] Ruben JD, Davis S, Evans C, et al. The effect of intensity-modulated radiotherapy on radiation-induced second malignancies. Int J Radiat Oncol Biol Phys 2008;70:1530–6.
[7] Rothkamm K, Horn S. ΓH2AX as protein biomarker for radiation exposure. Ann Ist Super Sanità 2009;45:265–71.
[8] Thierens H, Vral A, van Eijkeren M, Speleman F, De Ridder L. Micronucleus induction in peripheral blood lymphocytes of patients under radiotherapy treatment for cervical cancer or Hodgkin's disease. Int J Radiat Biol 1995;67:529–39.
[9] Werbrouck J, De Ruyck K, Beels L, et al. Prediction of late normal tissue complications in RT treated gynaecological cancer patients: potential of the γ-H2AX foci assay and association with chromosomal radiosensitivity. Oncol Rep 2010;23:571–8.
[10] Vandersickel V, Depuydt J, Van Bockstaele B, et al. Early increase of radiation-induced γH2AX foci in a human Ku70/80 knockdown cell line characterized by an enhanced radiosensitivity. J Radiat Res 2010;51:633–41.
[11] Willems P, August L, Slabbert J, et al. Automated micronucleus (MN) scoring for population triage in case of large scale radiation events. Int J Radiat Oncol 2010;86:2–11.
[12] Faul F, Erdfelder E, Buchner A, Lang AG. Statistical power analyses using G∗Power 3.1: tests for correlation and regression analyses. Behav Res Methods 2009;41:1149–60.
[13] Ost P, Speleers B, De Meerleer G, et al. Volumetric arc therapy and intensity-modulated radiotherapy for primary prostate radiotherapy with simultaneous integrated boost to intraprostatic lesion with 6 and 18 MV: a planning comparison study. Int J Radiat Oncol Biol Phys 2011;79:920–6.
[14] Aznar MC, Petersen PM, Logadottir A, et al. Rotational radiotherapy for prostate cancer in clinical practice. Radiother Oncol 2010;97:480–848.
[15] Butterworth KT, McGarry CK, Trainor C, et al. Out-of-field cell survival following exposure to intensity-modulated radiation fields. Int J Radiat Oncol Biol Phys 2011;79:1516–22.
[16] Beels L, Werbrouck J, Thierens H. Dose response and repair kinetics of gamma-H2AX foci induced by in vitro irradiation of whole blood and T-lymphocytes with X- and gamma-radiation. Int J Radiat Oncol Biol 2010;86:760–8.
[17] Mancuso M, Pasquali E, Leonardi S, et al. Oncogenic bystander radiation effects in *Patched* heterozygous mouse cerebellum. PNAS 2008;105:12445–50.
[18] Bonassi S, Znaor A, Ceppi M, et al. An increased micronucleus frequency in peripheral blood lymphocytes predicts the risk of cancer in humans. Carcinogenesis 2007;28:65–631.